COMPUTATIONAL MODELING OF HEAT TREATING PROCESSES BY USE OF HT-MOD AND ABAQUS

G. SÁNCHEZ SARMIENTO[†,‡], A. GASTÓN[§] and G. TOTTEN[*]

† *Facultad de Ingeniería, Universidad de Buenos Aires, Av. Paseo Colón 850, 1063 Buenos Aires, Argentina*
gustavo.sarmiento@kbeng.com.ar
§ *CIC-UNR, FCEIyA, Universidad Nacional de Rosario, Av. Pellegrini 250, 2000 Rosario, Argentina*
analiag@fceia.unr.edu.ar
‡ *Universidad del Salvador, Facultad de Ciencia y Tecnología, Buenos Aires, Argentina*
* *Portland State University, Portland, OR, USA. totten@cecs.pdx.edu*

***Abstract*— This paper presents an overview of mathematical approaches for modeling heat treating process, mainly concerned by coupling heat conduction with phase transformation, prediction of microstructure and material hardness, as well as estimation of heat transfer coefficients. The program HT-mod developed by the authors is briefly described. An analysis of distortions and residual stresses by a combination of HT-mod and ABAQUS Software is outlined. The performance of vegetable oils (castor, soybean and mineral oil) as quenchants are summarized as an application example. Comparison between measured and predicted hardness and microstructure of AISI 4140 bars is provided for validation of the methodology proposed for modeling heat treating processes. On average, good agreement was obtained.**

***Keywords*— heat treatment, steels, numerical simulation, microstructure, optimization.**

I. INTRODUCTION

Heat treatment is an integral part of the manufacturing processes of today's steel components. A heat treatment cycle will typically involve heating up and cooling down components. Both aspects of the cycle affect the shape, geometry, microstructure and mechanical state of the components in the sense that they will cause the component to expand and contract. The thermal stresses induced by the resulting temperature gradient may be large enough to cause fracture of the part, or to exceed the elastic limit resulting in permanent residual stresses and gross distortions in the component.

Computer simulation has become a powerful tool for analysis, assisting in the design and optimization of heat treating processes to achieve the desired as-quenched and tempered mechanical properties of steel. Computational modeling deals with coupled phenomena of heat transfer, phase transformation, electromagnetic induction, diffusion of carbon and other chemical elements within the matrix, as well as thermo mechanical behavior of components in response to a heat treatment. A literature review regarding modeling and simulation in this field was presented by Totten *et al.* (2004).

Heat treatment of steel involves heating the steel to an elevated temperature, typically the austenitizing temperature, often with subsequent quenching into a vaporizable liquid medium such as water, oil or aqueous polymer quenchant. Figure 1 is a typical cooling curve which shows the three most common heat transfer mechanisms observed during conventional immersion cooling in water. Upon initial immersion, the part is surrounded by a vapor film where full-film boiling or vapor-blanket cooling occurs. When the temperature decreases to the Leidenfrost temperature, the vapor film (vapor blanket) collapses and surface wetting by the liquid occurs by a nucleate boiling process due to lateral heat conduction relative to the surface. When the surface temperature decreases to a temperature less than the boiling point, nucleate boiling ceases and convective cooling begins.

Cooling power of liquid quenchants can be expressed by using cooling curve data of standard probes, like JIS silver probe or ISO INCONEL 600 probe (Totten and Clinton, 1993). For the computer simulation of heat treating processes, accurate values of heat transfer coefficients (HTC) or heat fluxes must be provided as boundary values conditions at the surface of the workpiece. These parameters are estimated from cooling curves data by use of *a lumped-heat-capacity metho*d or by *an inverse method*. The first one is suitable for estimating HTC from JIS silver probe data (Bi< 0.1, Biot number), and the second one from ISO INCONEL 600 probe data (Biot number > 0.1) (Narazaki *et al.*, 1998; Chen *et al.*, 1997).

This paper presents a review of the work developed by the authors for modeling heat treating process, mainly dealing with the coupling between heat conduction, phase transformation, prediction of microstructure and material hardness as well as the estimation of HTC by use of the *inverse method* applying the Finite Element Software **HT-Mod** (Heat Treating Modeling)**.**

HT-Mod was applied to estimate the heat transfer coefficients of a wide variety of quenchants, like polyalkylene glycols and UCON solutions (Sánchez Sarmiento *et al.*, 1996a, b). Recently, Penha *et al.* (2005, 2006) studied the effect of fresh and used mineral oil and bath temperatures (40, 60, 80 and 100°C) on cooling time-temperature performance of a Inconel 600

probe. Canale *et al.* (2004, 2005a) extended this study to castor and soybean oil, and evaluated the effect of vegetable oil oxidation on the ability to harden AISI 4140 (Canale *et al.*, 2005b).

II. HEAT TRANSFER MODEL

A. Equations governing heat transfer during quenching

The main objective is the numerical calculation of the time and spatial distribution of the temperature, within a specimen during the heating and cooling process, coupled with the progress of microstructure transformation of austenite to ferrite, pearlite, bainite and martensite. The following unknown functions must be determined:

$T(\vec{r},t)$: probe temperature $\quad \vec{r} \in \Omega ; t \in \left[0; t_f\right]$;

$X_F(\vec{r},t)$: volume fraction transformed into ferrite;

$X_P(\vec{r},t)$: volume fraction transformed into pearlite;

$X_B(\vec{r},t)$: volume fraction transformed into bainite;

$X_M(\vec{r},t)$: volume fraction transformed into martensite.

The heat conduction equation to be solved is:

$$\nabla\cdot\left(k(\vec{r},T)\cdot\nabla T\right)+Q(T,\vec{r},t)=c(\vec{r},T)\,\rho(\vec{r},t)\,\frac{\partial T}{\partial t} \qquad (1)$$

where $k(\vec{r},T)$, $c(\vec{r},T)$, $\rho(\vec{r},t)$ denote respectively the thermal conductivity, the specific heat and the density of the material. $T(\vec{r},t)$ is subjected to the initial condition:

$$T\left(\vec{r},t=0\right)=T_0\left(\vec{r}\right); \quad \vec{r}\in\Omega \qquad (2)$$

with the following boundary conditions at the surface of the steel probe:

$$-k\frac{\partial T}{\partial n}=h_i\left(T-T_{qu}\right) \quad on\ \Gamma_i,\ i=1,\cdots,p \qquad (3)$$

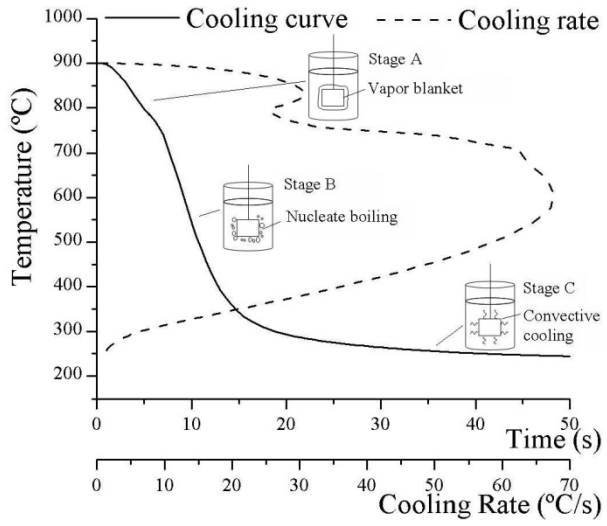

Figure 1. Cooling stages during quenching

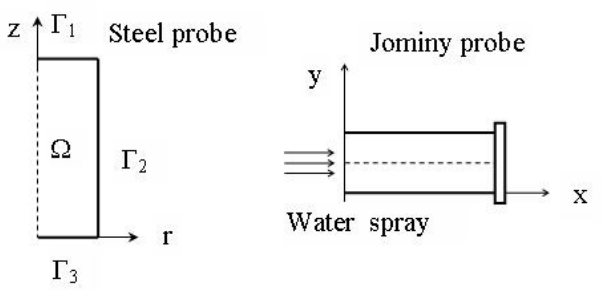

Figure 2. Calculation domains.

where $h_i(T)$ are the heat transfer coefficients corresponding to different portions of the boundary Γ and T_{qu} the quenchant temperature. Each one of these p cooling zones has a time dependent heat transfer coefficient that varies strongly along each partial boundary, depending on the heat transfer mechanism (vapour blanket, nucleate boiling, convective cooling) that governs the energy flow (Fig. 1).

$Q(T,\vec{r},t)$ represents the heat generation per unit volume owing to micro-structural transformations and takes the form:

$$Q\left(T,\vec{r},t\right)=\rho\left(\sum_{k=1}^{4}H_k(T)\frac{dX_k}{dt}\right) \qquad (4)$$

where X represents volume fraction austenite transformed to the phase k (k = 1, ferrite; 2, pearlite; 3, bainite; 4, martensite) and $H_k(T)$, the corresponding heat of transformation.

The solution of this set of equations is based on the finite element method for the discretization of the two-dimensional domain (Cartesian and symmetry of revolution systems), and a Crank-Nicholson finite difference scheme for the time variable. The procedure is standard and can be found in specific literature (Cook *et al.,* 1989; Zienkiewicz and Taylor, 1989). Figure 2 shows the different domains where the heat conduction problem is solved.

B. Mathematic modeling of phase-transformation during quenching

The phase-transformations during quenching can be classified into diffusion and non-diffusion type transformations and are governed by isothermal transformation diagrams (TTT-diagrams).

For the given steel grade, the diffusion-type transformation from austenite to ferrite/pearlite/bainite is modeled by the Johnson–Mehl-Avrami (JMA) kinetic equation (Johnson and Mehl, 1939). The temporal evolution of each volume fraction may be represented by:

$$X_k(\theta)=f_{maxk}\left\{1-exp\left[-a_k\,\theta^{b_k}\right]\right\} \qquad (5)$$

where X_k is the volume fraction of austenite transformed into k^{th} phase, f_{maxk} the maximum volume fraction of phase k that can be transformed at that temperature, a_k and b_k kinetic parameters generally dependent on temperature and phase k.

The Johnson–Mehl–Avrami equation is only valid for isothermal transformations. In order to calculate the phase transformations by JMA equation and TTT

curves, cooling curves are regarded as a series of small isothermal time steps connected by instantaneous temperature changes following constant volume fraction lines (Prakash *et al.*, 1980), as depicted in Fig. 3.

In Eqns (5), θ is a virtual time that bears no relationship to real process time t, and represents the time taken to achieve a given volume fraction of austenite transformed under isothermal conditions. For continuous cooling, the transformation start from one phase to the other must be determined in order to express θ in terms of the variable t. The virtual time θ^* to obtain at T_{n+1} the same volume fraction X_n as in the previous time step n, is calculated according to (see Fig. 3):

$$\theta^*_{n+1} = \left[-\frac{ln\left(1 - X_n / f_n\right)}{a_k\left(T_{n+1}\right)} \right]^{\frac{1}{b_k(T_{n+1})}} \qquad (6)$$

The virtual time θ^* is incremented by Δt in order to calculate the volume franction transformed at the end of time step $n+1$ as follows:

$$\theta_{n+1} = \theta^*_{n+1} + \Delta t_{n+1} \qquad (7)$$

$$X_{n+1} = f_{n+1} \left\{ 1 - exp\left[- a_{n+1}\left(T_{n+1}\right) \theta^{b_{n+1}} \right] \right\} \qquad (8)$$

The diffusionless transformation from austenite to martensite is calculated by using the equation proposed by Koistinen and Marburger (1959):

$$X_M(\theta) = \left(1 - X_F - X_P - X_B\right)\left\{1 - exp\left[-c_M\left(M_S - T\right)\right]\right\} \qquad (9)$$

where c_s is a constant and M_s the martensite start temperature, which depends on the steel grade.

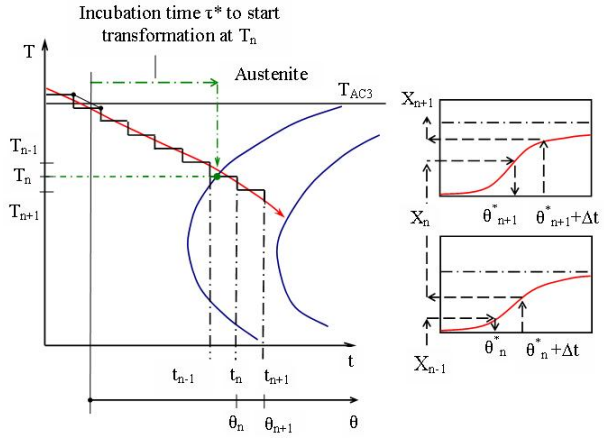

Figure 3. Cooling curve approximation superimposed on TTT Diagram. Relation between t and θ variables.

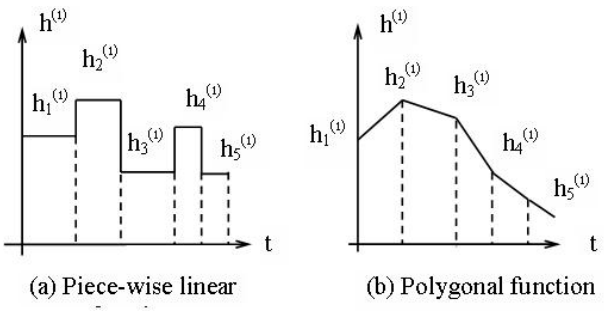

Figure 4. Heat transfer coefficient time approximations

C. Estimation of heat transfer coefficients

In heat treating processes the energy is removed from the surface of the part by convection and/or radiation. In some cases, the heat transfer coefficients are not known in advance and in others it is desired to optimize their values in order to make the treated part undergo a prescribed thermal evolution. Provided that the temperature change inside the component and on its surface are measured, it is possible to solve the inverse heat transfer problem to determine the time variation of the heat transfer coefficients, that best satisfies productions demands. The time dependence of the heat transfer coefficient can be approximated by piece-wise linear or polygonal functions, each one defined by a set of parameters $h_i^{(r)}\left(r = 1, \cdots, p \; ; \; i = 1, \cdots, q\right)$ as shown in Fig. 4.

On calling T_k^m , the measured temperature, and T_k^c, the numerically calculated temperature at those points, one can pose the problem of obtaining the values of the heat transfer coefficients h_i that minimize the function:

$$S = S\left(h_i^{(r)}\right) = \sum_{k=1}^{n} \left(T_k^m - T_k^c\right)^2 = mín \qquad (10)$$

n being the total number of measured temperatures, i.e the number of points times the number of measurements at each point.

The algorithm to solve the inverse problem is presented in detail in Sánchez Sarmiento *et al*. (1998).

D. Hardness prediction model

The procedure to predict the hardness distribution of a heat treated steel specimen taking into account the influence of its chemical composition, is based on the assumption that the hardness is a direct function of the thermal history undergone during the quenching process (Totten and Clinton, 1993). The methodology proposed is outlined below and shown in Fig. 5:

1. The hardenability of a Jominy probe, with the same chemical composition of the steel specimen to be treated, is calculated according to SAE Standard J406 (SAE Standard, 1985).
2. The spatial and temporal distribution of the temperature within the Jominy probe during the quenching test coupled with the phase change transformation process is obtained according to section A.
3. A similar calculation considering the specific heat treating process (quenching, induction heating) is carried out for the component.
4. After solving these two thermal problems, cooling curves corresponding to any nodal point of the Jominy probe and of the steel specimen are available. To assign a hardness value to a specimen nodal point, its cooling curve is compared to all the cooling curves of the Jominy points. Once the Jominy point with the closest cooling curve is identified, its hardness is assigned to the specimen point. In this way, the hardness of the Jominy probe is mapped into the steel bar. On using these hardness nodal values, hardness distribution contours for the component can be obtained.

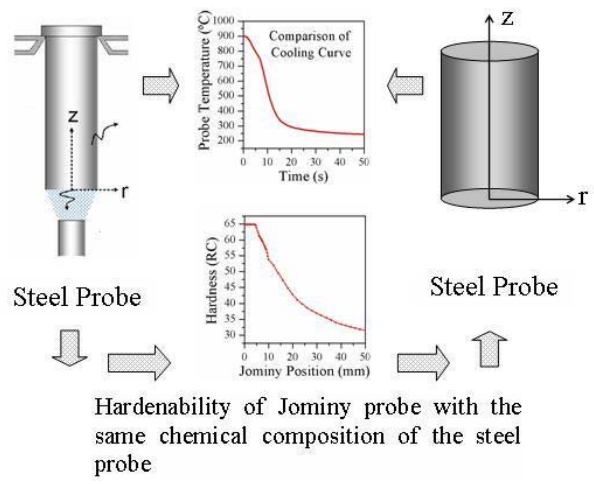

Figure 5. Hardness prediction (SAE Standard J406).

E. HT-Mod Programme. Software Capabilities

The basic steps performed by the program are briefly outlined here:

1. User specification through interactive menus of:
- Geometrical data of the steel probe
- Thermal properties of the steel probe
- Chemical composition of the steel probe
- TTT diagram data of the steel probe
- Phase transformation data of the the steel probe
- Austenitization temperature
- Heat transfer coefficients (HTC) as function of time
- Thermocouples location and measured temperatures in the steel probe for estimation of HTC
- Time steps for numerical simulation and output graphic options

2. Automatic mesh generation of the domain.
3. Solution of the heat balance equation of Jominy and steel probe
4. Estimation of HTC (optional)
5. Determination of hardness distribution
6. Post-processing. Results are shown in different graphical formats: isotherms for time steps specified by the user, time temperature evolution of user specified nodes superimposed on TTT diagram; time evolution at user specified nodes of volume fraction transformed (austenite, ferrite, pearlite, bainite, martensite), phase transformed isolevels, hardness distribution.

F. HT-Mod + ABAQUS Programmes.

Heat treatment processes, particularly quenching, are essential to improve mechanical properties in the production of steel castings, but they also generate residual strains and stresses as well as volumetric expansion due to phase transformations and microstructure changes of a steel body.

A reliable evaluation of the cooling power of quenchants is relevant for the computer simulation of heat treating processes. A heat flux or heat transfer coefficient is used as the boundary condition to simulate the cooling process of the workpieces and accurate values must be provided.

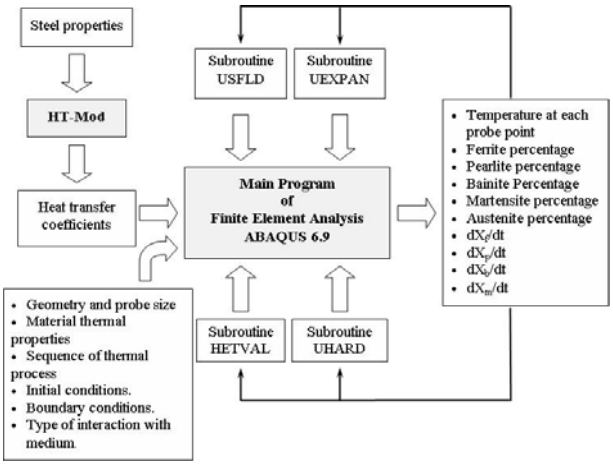

Figure 6. General scheme for modeling heat treatment process with HT-MOD +ABAQUS**.**

A very efficient sequential combination of HT-Mod and the general Finite Element Analysis Software **ABAQUS** (Dassault Systèmes Simulia Corp., 2007) provides a powerful tool for calculation of distortion and thermal stresses during heat treating processes. The general scheme of this combination is given in Figure 6.

ABAQUS solvers do not consider metallurgical and micro-structural behavior of steel materials by themselves, but it is possible to extend the functionality of **ABAQUS** models performing modifications or optimizations (customization) by FORTRAN subroutines.

A package of subroutines were developed in order to solve the coupled problem and to calculate all the microstructures resulting from quenching (ferrite, pearlite, bainite, and martensite volume fractions), depending on the cooling rate:

USDFLD: Gives the transformed volume fraction of austenite into ferrite, pearlite, bainite and martensite.

HETVAL: Gives the heat generated by each one of the phase transformations.

UEXPAN: Gives the volume change due to temperature variation and the phase transformations.

UHARD: Gives the yield stress for the temperature and volume fractions of each phase at each integration point

G. Macro Calorimeter Method.

In Section **C**, the estimation of heat transfer coefficients based on the temperature evolution measured by thermocouples inserted in the probe was described. However, when treating specimens of large size (large casting of crack sensitive steel alloys), collecting the experimental data can be a very time-consuming and labor intensive work.

Recently, Kuyucak *et al.* (2005a, b) presented an alternative procedure to characterize the cooling power of a quenchant. Instead of using thermocouple-probe assemblies, this process involves the measurement of the increase of the water temperature in the quenching tank as a function of time as if the quench tank were a macro-calorimeter. From this data, heat flux from the steel probe to the quenchant can be estimated and then used to predict microstructure and hardness.

The following assumptions are made to model the

quenching process:

1. The quenchant temperature is uniform as a result of intense agitation.
2. Convection and radiation heat transfer to the room is negligible during the quenching test.
3. Heat is transferred by conduction within the probe.
4. Heat flow from the probe to the quenchant by radiation and conduction through the lateral, top and bottom surface of the probe is uniform

A calorimetric energy balance may be stated as:

$$m_{qu}c_{qu}\left(\overline{T}_{qu}(t)-\overline{T}_{qu}(0)\right)=\int_0^t q_p(t)\,A_t\,dt \qquad (11)$$

where m_{qu} is the total mass of the quenchant; c_{qu} is the specific heat of the quenchant; $T_{qu}(t)$ is the temperature of the quenchant as a function of the time t; $q_p(t)$ is the heat flux assumed uniform at all the surface of the probe; and A_t is the total area of the probe.

From Eq. (12) an expression for the heat flux transferred from the probe to the quenchant can be derived if the evolution of the mean temperature of the bath is known (measured):

$$q_p(t)=\frac{m_{qu}c_{qu}}{A_t}\frac{dT_{qu}(t)}{dt} \qquad (12)$$

where m_{qu} is the total mass of the quenchant; c_{qu} is the specific heat of the quenchant; $T_{qu}(t)$ is the temperature of the quenchant as a function of the time t; $q_p(t)$ is the heat flux assumed uniform at all the surface of the probe; and A_t is the total area of the probe.

The temperature evolution, microstructure and hardness within the probe can be predicted by solving Eq. (1) subjected to the Neumann boundary condition (13) that results from applying the heat flux (12) at the surface of the probe in contact with the quenchant:

$$-k\frac{\partial T}{\partial n}=q_p \qquad on\ \Gamma_i,\ i=1,\cdots,p \qquad (13)$$

Minor modifications were introduced in HT-Mod to simulate a quenching process with the Calorimetric Method.

III. APPLICATION EXAMPLES AND MODEL VALIDATION

As an application example, some of the results obtained in the study of the performance of different vegetable oil as quenchants will be presented. A detailed description is given in (Canale *et al.,* 2004, 2005a, b; Penha *et al*., 2005, 2006). Fresh and oxidized sample of castor oil, soybean oil and a mineral oil (MC1) were considered as quenchants using the Inconel 600 probe described in ISO 9950. Cooling curves (*T-t*) were obtained using a Type K thermocouple inserted to the geometric center of the 12.5 mm dia x 60 mm cylindrical probe. Bath temperature was set to 40ºC. Heat transfer coefficients were estimated with **HT-Mod**.

Figure 7 shows the calculated heat transfer coefficients as a function of temperature, comparing the quenching power of the six quenchants.

The estimated heat transfer coefficients of the fresh and used quenchants confirm that oxidation of uninhibited castor oil and soybean oil produced greater impact on the heat transfer properties compared to the mineral oil (MC1) quenchant.

Based on the heat transfer coefficients obtained with **HT-Mod, ABAQUS** was used to simulate the distortion and the residual stresses produced in the Inconel 600 probe, by solving the corresponding thermal-elastic-plastic problem. Note that no phase transformation occurs in Inconel 600 during quenching, therefore there are no transformation-induced stresses. Taking advantage of symmetry, only a quarter of the Inconel probe was modeled, using a finite element mesh containing 11 nodes along the radial direction and 21 nodes along the longitudinal direction.

Inconel 600 probe, distortion and spatial distribution of the hoop stress at the end of quenching are shown in Fig. 8 for new castor oil. Displacements were multiplied by a factor 70. N_1 is the node at the core and N_{11} at the surface.

Figure 9 shows longitudinal and hoop stresses, at nodes located at the middle plane of the probe, along the radial direction. Residual stresses are tensile in core and compressive in surface

Maximum values and residual stresses computed for the six quenchants are presented in Table 1. These results showed that fluid oxidation (used) produced a substantial increase in residual stresses and distortion when compared to fresh fluids for soybean and mineral oil, while the opposite trend was obtained for castor oil.

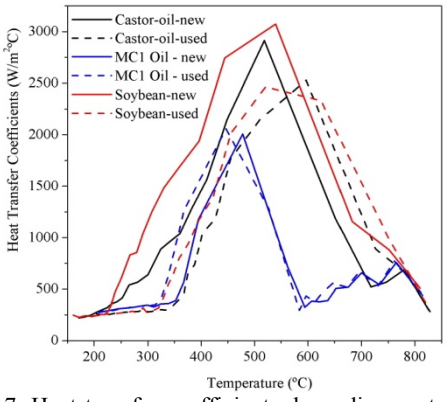

Figure 7. Heat transfer coefficients depending on temperature estimated by HT-Mod for the six quenchants

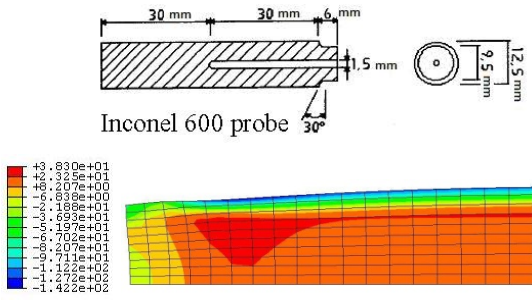

Figure 8. Distortion and hoop stress in MPa distribution at end of quenching for new castor oil. N1(core); N_{11} (surface).

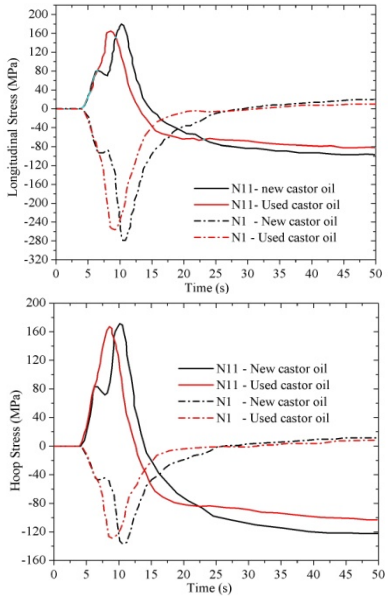

Figure 9. Longitudinal and hoop stresses for new and used castor oil. Nodes located at the middle plane, along radial direction. N_1 (core), N_{11}(surface)

Table 1. Comparison of longitudinal, hoop and residual stresses for fresh and used quenchants.

	Castor oil		MC1 oil		Soybean oil	
	Fresh	Used	Fresh	Used	Fresh	Used
Max σ_z [MPa]	180	172	180	180	180	180
Max σ_θ [MPa]	176	170	183	183	183	175
Residual σ_z [MPa]	-99	-80	$\lvert\sigma_z\rvert$<5	$\lvert\sigma_z\rvert$<5	$\lvert\sigma_z\rvert$<5	-90
Residual σ_θ[MPa]	-123	-104	$\lvert\sigma_\theta\rvert$<5	$\lvert\sigma_\theta\rvert$<5	$\lvert\sigma_\theta\rvert$<5	-111

The methodology described in Section **D** to predict steel hardeness by use of SAE Standard J406 was applied to model a wide variety of heat treating processes and extended to analyze other industrial applications like induction heating, hot rolling, quenching and tempering of stainless steels (Sánchez Sarmiento *et al.* 1997, 1999). Validation of this procedure was carried out by comparison of predicted and measured hardness values in quenched probes of different steel grade and chemical composition. Figure 11 compares measured and predicted hardness profiles for SAE 1040 steel bars. The bars were treated by induction heating and a detail description of the evaluation of the heat source owing to Eddy currents (Joule effect) is given in (Sánchez Sarmiento *et al.*, 1998). Figure 10 shows the ability of the model to detect the changes in hardness profiles and case depth (surface area where the microstructure is, i.e. 50% martensite) owing to differences in chemical composition.

Finally, the use of the Calorimetric Method to predict the as-quenched hardness of a medium alloy steel (AISI 4140) when quenched into water will be summerized (Gastón *et al.*, 2008).

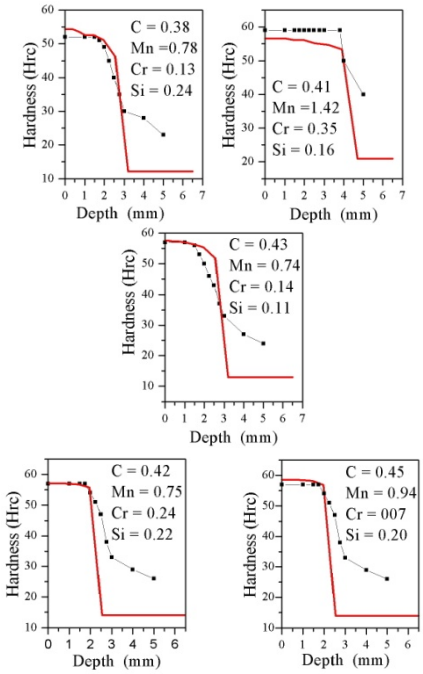

Figure 10. Comparison between measured and predicted hardness profiles for SAE 1040 steel bar with different chemical compositions. Measured values (■)

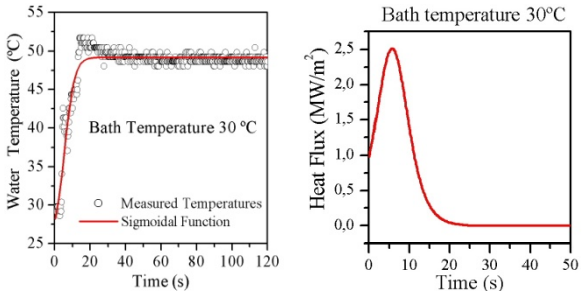

(a) (b)

Figure 11. 4140 steel bars quenched in water at 30ºC. (a) Measured water temperature and fitted sigmoidal function;(b) Estimated heat flux

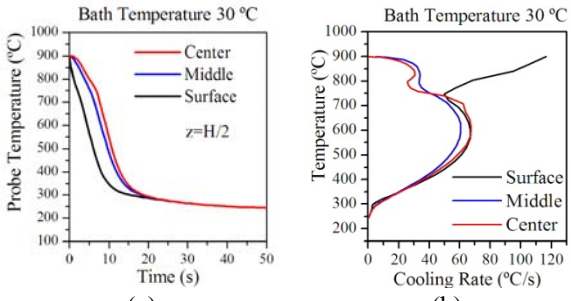

(a) (b)

Figure 12. Simulation results for 4140 steel quenched in water (30ºC)

Figure 11a shows measured bath temperature and fitted sigmoidal curve for quenching 4140 steel bars in water at 30ºC. Estimated heat flux for solving the heat transfer problem (Eqns. 1 and 13) is plotted in Fig. 11b.

Cooling curves at three points along the radial coordinate (center, middle, surface) at mid height of the probe are plotted in Fig. 12a and the corresponding cooling rates in Fig. 12b.

Measured and predicted hardness of 4140 steel bars quenched in water at 30ºC and 45ºC are shown in Fig. 13. Excellent agreement between calculated and experimental hardness distribution were obtained, as the greatest mismatch between them is 3 HRC.

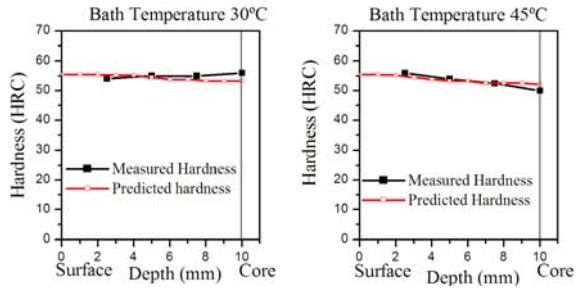

Figure 13. Comparison between measured and predicted hardness for 4140 steel quenched in water

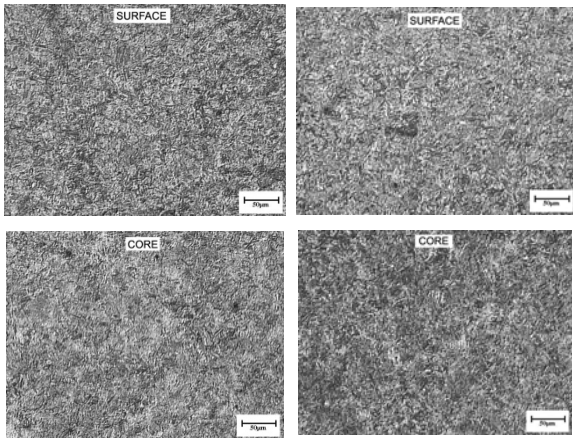

(a) (b)

Figure 14. Microstructure of 4140 steel bars quenched in water (a) at 30°C (b) at 45°C. Surface and core samples

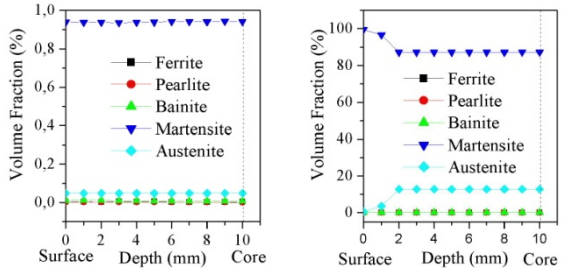

(a) (b)

Figure 15. Predicted microstructure along radial direction 4140 steel bars, in water (a) at 30°C (b) at 45°C

Finally, measured and predicted microstructures are shown in Fig. 14 and 15, respectively. Microstructures were determined using Philips XL -30 scanning microscope by 2000X magnification according to ASTM E883-02 Standard Guide for Reflected–Light Photomicrography. Metallographs exhibited martensitic microstructure at the core and surface of 4140 steel bars. Figure 15 shows predicted phase volume fractions along the radial direction of the steel bar. It can be concluded that the predicted microstructure is in good agreement with the experimentally measured results.

IV. CONCLUSIONS

An overview of the mathematical approaches for modeling heat treating process is described in this paper, focusing on the coupling between heat conduction with phase transformation and the prediction of the material hardness.

The codes developed allow sensitivity analysis of process parameters that are relevant to achieve the desired as-quenched and tempered mechanical properties of steel with a heat treating process.

This work illustrates potential benefits of computational simulation to investigate the impact of different quenchants and quenching conditions on a heat treatment process.

Also, the potential of the Macro Calorimeter Method as a viable method for obtaining cooling curve data without the use of thermocouples inserted in a workpiece and predicting the as-quenched hardness of steel (AISI 4140) was illustrated.

NOTATION

A_t	total steel probe heat transfer area (m^2)
c	specific heat of steel probe (J/kg ºC)
c_{qu}	specific heat of quenchant (J/kg ºC)
Bi	Biot number, $Bi = hL/k$
L	characteristic dimension of the steel probe
h_i	heat transfer convective coefficient on Γ_i (W/m^2 ºC)
H_i	heat of transformation from austenite to phase i= F, P, M (J/kg)
k	thermal conductivity of steel probe (W/mºC)
m_{qu}	total mass of the quenchant (kg)
n	outward normal
N	shape function
q_p	heat flux at surface probe (W/m^2)
Q	heat generation per unit volume owing to micro-structural transformations (W/m^3)
S	sum of square differences between measured and calculated steel probe temperatures ($ºC^2$)
t	time (s)
T	steel probe temperature (ºC)
T_0	initial steel probe temperature (ºC)
T_k^c	calculated steel probe temperature (ºC)
T_k^m	measured steel probe temperature (ºC)
$\overline{T}_{qu}$	mean quenchant temperature (ºC)
r	radial coordinate
X_i	volume fraction of austenite transformed to phase i= Ferrite, Pearlite, Bainite, Martensite

Greek Symbols

Γ_i	boundary i of steel probe
ρ	steel probe density (kg/m^3)
ρ_{cu}	quenchant density (kg/m^3)
ν	coefficient of JMA equation (s^{-1})
θ	virtual time (s)

REFERENCES

Canale, L.C.F., G.S. Sarmiento; G.E. Totten and R. N. Penha, “Characterization of the Surface Temperatures and Heat Transfer Properties of Fresh and

Used Vegetable Oils Relative to Mineral Oil Using HT-MOD and Abaqus," *Proc. Cuarta Reunión Argentina de Usuarios de ABAQUS*, San Carlos de Bariloche, Argentina, 21-43 (2004).

Canale L.C.F, A.C. Canale, M.R. Fernandes, S.C.M. Agustinho, G.S. Sarmiento and G.E. Totten, "Evaluation and impact of oxidative stability on the quenching performance of castor oil and soybean oil," *Proc. of 2nd International Conference on Heat Treatment and Surface Engineering in Automotive Applications*. Eds. S. Gallo, B. Liscic and P.L. Antona, Riva Del Garda, Italy, Associazione Italiana di Metallurgia, Milano, Italy, Paper No. 010 (2005a).

Canale, L.C.F, G.S. Sarmiento, G.E. Totten and R. N. Penha, "Effect of vegetable oil oxidation on the ability to harden AISI 4140 Steel," *Proc. of 60 Congresso Anual da Associação Brasileira de Metalurgia e Materiais,* Belo Horizonte, 3209-3217 (2005b).

Chen, X., L. Meekisho, M. Becker and G.E. Totten. "Numerical Validation of Lumped Capitance Analysis for Deriving heat Transfer Coefficient Using Quenching Probe," *17th ASM Heat Treating Society Proceeding,* Indianapolis, USA, 355-361 (1997).

Cook R., D. Malkus and M. Plesha, *Concepts and applications of finite elements analysis*, John Wiley & Sons (1989).

Dassault Systèmes Simulia Corp. *ABAQUS/CAE, User's Manual, Version 6.7*. Providence, Rhode Island (2007).

Gastón, A., G. Sánchez Sarmiento, R.M. Muñoz Riofano, L.C.F. Canale, G. E. Totten, and I. Felde "Modeling Steel Quenching by the Calorimeter Method," *Proc. Mechatronikai és Biztonságtechnikai Szimpózium*. Budapest, Hungary (2008).

Johnson, A.W. and R.F. Mehl, "Reaction kinetics in processes of nucleation and growth," *Trans. AIME* **135,** 416–425 (1939).

Koistinen, D.F. and R.E. Marburger, "General equation prescribing the extent of the austensite transformation in pure iron-carbon alloys and plain carbon steels," *Acta Metall.,* **7,** 50–60 (1959).

Kuyucak, S., P. Newcombe, P. Bruno, R. Grozdanich and G. Looney, "Quench time measurement: as a process control tool, part I," *Heat Treating Process*, January/February, 60-63 (2005a).

Kuyucak, S., P. Newcombe, P. Bruno, R. Grozdanich and G. Looney, "Quench time measurement: as a process control tool, part II," *Heat Treating Process*, March/April, 42-44 (2005b).

Narazaki, M., M. Kogawara, A. Shiravori and S. Fuchizawa, "Accuracy of evaluation methods for heat transfer coefficients in quenching," *Proc. of 18th Conference ASM International Heat Treating Society,* Rosement, USA, 509-517 (1998).

Penha, R.N., L.C.F. Canale, G.E Totten, Sarmiento G.S. and J.M. Ventura "Simulation of heat transfer and residual stresses from cooling curves obtained in quenching studies," *Journal of ASTM International*, **3**, 1-14 (2005).

Penha, R.N., L.C.F. Canale, G.E Totten and G.S. Sarmiento, "Simulation of heat transfer properties ant thermal residual stress from quenching studies". *Revista Minerva*, **2**, 165-172 (2006).

Prakash, K., A. Garwaland and J.K. Brimacombe, "Mathematical model of heat flow and austenite - pearlite transformation in eutectoid carbon steel rods for wire," *Metall. Trans*., **12B**, 121-133 (1980).

SAE Standard, *Methods of determining hardenability of steels*- SAE J406 May (1985).

Sánchez Sarmiento, G., G.E. Totten, G. Websters and E. Mues, "Computational determination of film heat transfer coefficients of polyalkylene glycols bath solutions in quenching operations," *Proc. 16th Heat Treating Society Conf.*, ASM International, Cincinnati, Ohio, USA, 383-390 (1996a).

Sánchez Sarmiento, G., C. Barragán, E. Mues and C. Bun te, "Application of computer models to the determination of heat transfer coefficients of UCON quenchant solutions in heat treating operations," *Proc. 2nd International Conference on Quenching and the Control of Distorsion,* ASM International, Cleveland, Ohio, 275-281 (1996b).

Sánchez Sarmiento, G., A Gastón and J. Vega, "INDUCTER-B: A finite element phase transformation model of induction heat treating of steels sensitive to its chemical composition," *Proc. 1st International Conference on Induction Heat Treating, ASM Heat Treating Society*, Indianápolis, USA, 841-848 (1997).

Sánchez Sarmiento, G., A. Gastón and J. Vega, "Inverse heat conduction coupled with phase transformation problems in heat treating process," *Computational Mechanics - New Trends and Applications*, Barcelona, Spain. CD-Book. Part VI, Section 1, Paper 16 (1998).

Sánchez Sarmiento, G., J.C. Cuyás, A.I. Ledesma, M.A. Morelli and M.J.A. Solari, "TRATINOX, a finite element model of quenching and tempering of stainless steels," *Proc. 3rd International Conference on Quenching and Control of Distortion*, Praga, Check Republic (1999).

Totten, G.E. and N.A. Clinton. *Handbook of quenchants and quenching technology*, ASM International Materials Park, OH (1993).

Totten, G.E., K. Funatani and L. Xie. *Handbook of Mettallurgical Process Design*, Marcel Dekker IncNew York (2004).

Zienkiewicz, O.C. and R.L. Taylor, *The finite element method*, McGraw Hill (1989).

Received: December 28, 2009
Accepted: September 18, 2010
Recommended by Subject Editor: Walter Ambrosini